# Investigating population structure of bigeye tuna in the Indian Ocean using otolith chemistry

Naomi Clear[1], J. Paige Eveson[1], Audrey M. Darnaude[2], Maylis Labonne[2,] Iraide Artetxe-Arrate[3], Igaratza Fraile[3], Jessica Farley[1], Peter Grewe[1], Pratiwi Lestari[4], Muhammad Taufik[4], Achmad Zamroni[4], Asep Priatna[4], Jorden Aulich[1], Matt Lansdell[1], Hector Lozano-Montes[5], Leonid Danyushevsky[6], Zulkarnaen Fahmi[7], Wudianto[8], Hilario Murua[9,] Francis Marsac[10] and Campbell Davies[1].

[1] CSIRO Oceans and Atmosphere, Hobart, Tasmania, Australia
[2] Marbec, Univ Montpellier, CNRS, Ifremer, IRD, Montpellier, France
[3] AZTI, Marine Research, Basque Research and Technology Alliance (BRTA), Herrea Kaia, Portualdea z/g, 20110 Pasaia - Gipuzkoa, Spain
[4] Research Institute for Marine Fisheries, MMAF, Indonesia
[5] CSIRO Oceans and Atmosphere, Crawley, Australia
[6] Centre for Ore Deposit and Earth Sciences (CODES) and School of Earth Sciences, University of Tasmania, Hobart, Australia
[7] Research Institute for Tuna Fisheries, MMAF, Indonesia
[8] Centre for Fisheries Research, Indonesia
[9] International Seafood Sustainability Foundation, 1440 G Street NW, Washington, DC 20005, USA.
[10] Marbec, Univ Montpellier, CNRS, Ifremer, IRD, Sète, France

## Abstract

Natal origin and stock structure of bigeye tuna (*Thunnus obesus*) in the Indian Ocean were investigated using trace elements in otoliths. Otoliths were collected from (i) young of the year (YOY) bigeye caught in the west central and north east regions of the Indian Ocean, which are known to be spawning areas, and (ii) older fish in the south west and south east regions of the Indian Ocean. Otoliths were analysed by LA-ICP-MS at two points: near the core and at the edge, providing an elemental signal from material deposited while the fish were close to their spawning grounds and from material deposited while they were in or close to their capture areas, respectively. Twelve elemental isotopes were measured: Li, Na, Mg, P, K, Mn, Fe, Cu, Zn, Rb, Sr, Ba. Core and edge signatures for the same otolith were significantly different for most elements. Core signatures did not differ significantly for YOY bigeye in the west and east northern locations; this suggests that the ocean chemistry did not differ significantly between these locations. The core signatures for older fish in the west and east southern locations did not differ significantly from each other, but they did differ significantly from the core signatures observed for fish from the northern spawning locations, indicating either: (i) the fish from the southern locations were not spawned in either of the northern locations; or (ii) they were spawned in one of the northern locations but the ocean chemistry was very different in the years they were spawned. Core and edge signatures for the same otolith were significantly different and edge signatures also did not differ between fish from the two northern locations. While temporal variability in otolith elemental chemistry may confound spatial structure information, these results show that otolith chemistry can differentiate separate groups of bigeye within the Indian Ocean. Analysing YOY from known spawning areas over several years would set up a baseline for matching otolith cores from older fish collected in other areas of the Indian Ocean that may then provide evidence of population structuring.

## Introduction

In 2017, CSIRO (Australia) in collaboration with AZTI (Spain), IRD (France) and CFR (Indonesia) commenced a 3-year collaborative project on population structure of tuna, billfish and sharks of the Indian Ocean (PSTBS-IO) funded by the European Union and the consortium partners. The overall aim of the PSTBS-IO project was to develop a better understanding of the stock structure of tuna, billfish and sharks of the Indian Ocean using two independent, complementary techniques: genetics and otolith (or vertebrae) microchemistry. Here, we present the results from the bigeye tuna (BET) otolith microchemistry component of the PSTBS-IO project.

In the Indian Ocean, bigeye tuna is targeted mainly by the longline and purse seine fleets and the total annual catch is around 95,000 tonnes (IOTC, 2019). Bigeye tuna are capable of long-distance migrations (Fonteneau and Hallier 2015, Hallier and Fontenau 2015) while a high degree of site fidelity has also been reported (Evans et al. 2008, Fonteneau and Hallier 2015, Schaeffer et al. 2015). This variation in behaviour produces a complex spatial structure within an ocean basin, posing a challenge for sustainable management.

Otolith microchemistry can provide information on population structure and connectivity of a species, if fish have inhabited different environments with distinct physicochemical properties (Campana et al. 1999). Previous studies have used otolith microchemistry to determine natal origin and population connectivity of some tuna and billfish species (Artetxe-Arrate et al. 2019, Proctor et al. 2019, Rooker et al. 2007, 2016). The investigation of otolith microchemistry of bigeye tuna has thus far been limited to 2 studies. Proctor et al (2019) compared otolith stable isotopes and elemental chemistry of bigeye caught at nine sites in the Indonesian archipelago and two outlier sites, Maldives and Solomon Islands. Applying discriminant function analysis, individual fish were most often correctly classified to the location where they were captured, and when this was not the case, they were usually classified to adjacent or nearby locations, indicating fish had not moved large distances in their first 4 - 6 months of life. In a study in the Pacific Ocean, Rooker et al. (2016) found spatial variation in the otolith elemental and stable isotope signatures from young of the year (YOY) that were collected in four locations in the western and central Pacific Ocean. The stable isotope signatures were used as a baseline to classify age-1 to age 2+ fish to their natal origin by comparing the YOY signatures with otolith material from the older fish ablated near the core. In the current study, elemental signatures from the otolith cores and otolith edges from bigeye tuna were analysed to examine population structure. Signals from the core should reflect the fish's spawning origins and the otolith edge signals reflect the fish's known capture location.

## Methods

The bigeye otolith samples analysed were from four sampling locations (Fig. 1), referred to as Western Central Indian Ocean (WCI), North-East Indian Ocean (NEI), South-West Indian Ocean (SWI) and South-East Indian Ocean (SEI).

Due to sampling limitations, the samples from the different locations were collected during different periods (Table 1). All fish from the two northern sites (WCI and NEI) were age 0+ (24-44 cm fork length (FL)) and were substantially smaller than minimum size at maturity (see Zudaire et al. 2016). Fish from the two southern sites (SWI and SEI) were larger individuals (87-178 cm FL) (Fig. 1, Fig. 2, Table 1). The two northern locations are known spawning sites for bigeye (Nishikawa 1985, Stequert

and Marsac 1989, Suman et al. 2015), so the aim of the sampling design was to obtain a spawning ground signature for these locations and then see whether the core signatures from the adults sampled at the southern locations corresponded to either of these spawning sites.

The otoliths were analysed at the Centre for Ore Deposits and Earth Sciences (CODES) at the University of Tasmania using LA-ICP-MS, with a Resonetics RESOLution S-155 system with a Coherent 110 Compex Pro ArF excimer laser operating at 193nm wavelength and a ~20ns pulse width and an Agilent 7900 Inductively Coupled Plasma Mass Spectrometer (ICP-MS). The laser ablated 29-micron spots at 4 positions along the otolith from the core (earliest-deposited material) to the edge (the most recently deposited material). Twelve chemical elements were measured: 7Li, 23Na, 24Mg, 31P, 39K, 55Mn, 57Fe, 63Cu, 66Zn, 85Rb, 88Sr and 37Ba. Data reduction and processing was performed using LADR software (Norris and Danyushevsky 2018).

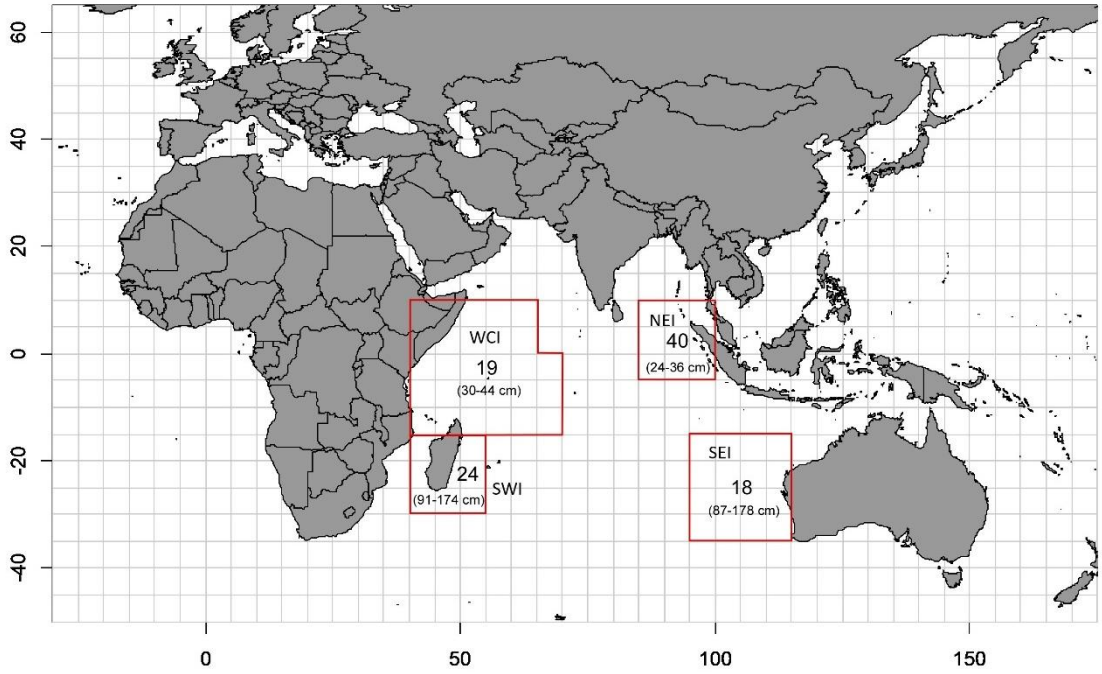


Figure 1. Map showing the number of bigeye otoliths analysed for each of four sampling locations, referred to as Western Central Indian Ocean (WCI), North-East Indian Ocean (NEI), South-West Indian Ocean (SWI) and South-East Indian Ocean (SEI); and the size range of fish at each location.

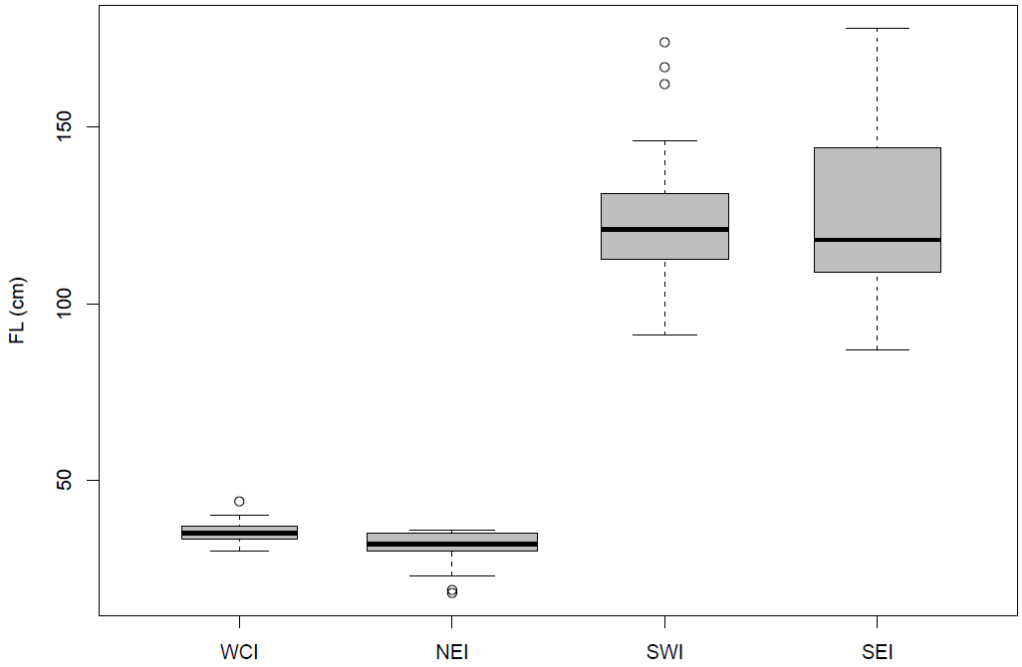


Figure 2. Boxplots of bigeye fork length (FL, cm) by sampling location, including only fish whose otoliths were selected for analysis.

Table 1. Number, sampling period, size range and estimated ages of fish for each of the sampling locations. Sizes are fork length (FL).

| **Location** | **N** | **Sampling dates** | **FL range (cm)** | ****Estimated age range (years)** |
|---|---|---|---|---|
| Western Central Indian Ocean (WCI) | 19 | February-April 2018 (primarily) | 30-44 | 0+ |
| North-East Indian Ocean (NEI) | 40 | April and November 2018 | 24-36 | 0+ |
| South-West Indian Ocean (SWI) | 24 | August-October 2017 (primarily) | 91-174 | 2-15 |
| South-East Indian Ocean (SEI) | 18 | May 2019 | 87-178 | 2-15 |

** based on length-at-age results from Eveson et al. 2015, Farley et al. 2006, Sardenne et al. 2015.

The spot near the core was examined to identify the chemical signatures deposited during the first weeks of life, which are most likely to reflect the fish spawning origins. Signatures from the otolith edge were also examined, since these data reflect the fish's known capture location, and can be used for validation purposes.

Several statistical analyses were performed on the elemental signatures from the core and from the edge. Principal component analyses (PCA) were used to determine which elements account for most of interindividual variability in the data, and to help visualize the data as this can be difficult with so many elements (using the dudi.pca function from the ade4 package in R). Since assumptions of normality and homoscedasticity were not met for all elements, permutational multivariate analyses of variance (PERMANOVA) were then carried out to test for differences in the multi-elemental signatures of fish among locations (using the adonis function from the vegan package in R). PERMANOVAs were performed using all elements, as well as only those elements that contributed significantly to interindividual variability in the data based on the PCAs. If the PERMANOVA

suggested signatures differed among locations, then subsequent pairwise tests were performed to determine which locations differed (using the pairwise.adonis function in R with Euclidean distance to calculate the similarity matrix and the Benjamini-Hochberg method for calculating the adjusted p-value). Note that prior to analyses, the data were log-transformed to reduce skewness and also standardised (i.e., for each element, the data was centred by subtracting the mean and scaled by dividing by the standard deviation).

## Results

Core and edge signatures for the same otolith were significantly different for most elements (Fig. 3). This is clear in the otolith data for the northern locations where, even though fish are assumed not to have undergone large-scale movements between spawning and capture, their core and edge signatures are still significantly different.

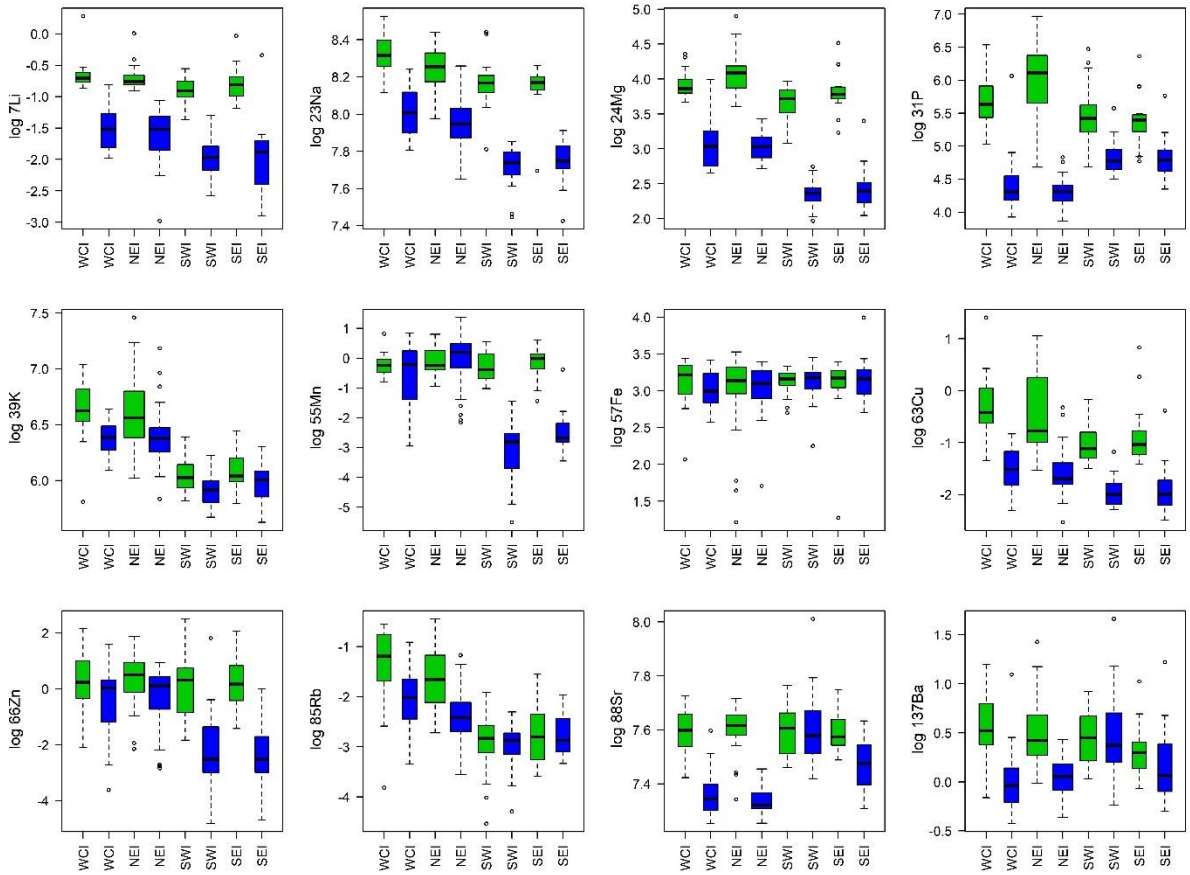


Figure 3. Boxplots comparing bigeye core (green) and edge (blue) signatures at the four sampling locations.

## Core results

Boxplots comparing core signatures between locations show that some elements are similar among all locations; however, for those elements that show clear differences (e.g. Mg, K, Rb), the two northern locations (NEI and WCI) appear similar to each other but different than the two southern locations (SEI and SWI) (Fig. 4).

The elements that contributed significantly to the interindividual variation in core signatures (>15% to axis 1 and/or 2 in the PCA) were Sr, Ba, Zn, Rb and K. (We originally used 20% as the criteria but this resulted in only one element (Sr), so we relaxed the criteria to 15% contribution). Results from PERMANOVAs run using all elements or just these five elements suggest that core signatures are not equal among all locations (p=0.001). Subsequent pairwise tests between locations show that this is due to the core signatures differing significantly between the two northern locations and two the southern locations (Table 2). Core signatures do not differ significantly between the two northern (spawning) locations, nor between the two southern locations (Table 2). Note that results using all elements are presented but that the conclusions are the same using just the subset of five elements. A biplot from the PCA showing individuals projected onto the first plane (i.e., the first two axes) helps to visualize these findings (Fig. 5).

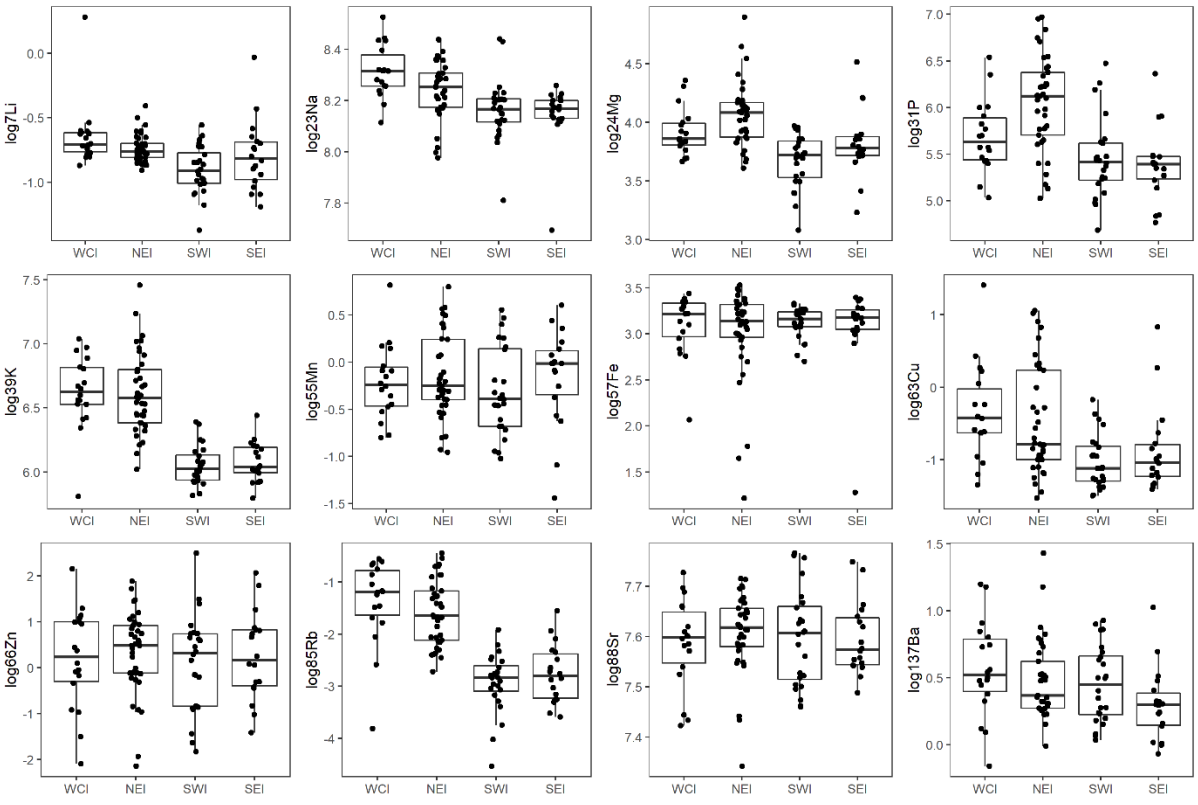


Figure 4. Boxplots comparing bigeye otolith core data between locations for each element. Note that the data have been log-transformed to reduce skewness and facilitate comparison.

Table 2. Results of pairwise comparisons of bigeye otolith core signatures between locations. In the Significance column, a blank means that the locations do not differ significantly at level 0.05, a dot (.) means they differ at level 0.05, and a star (*) means they differ at level 0.01.

| Pair | | | Df | Sum-of-Squares | F-statistic | R-squared | P-value | Adjusted P-value | Significance |
|---|---|---|---|---|---|---|---|---|---|
| WCI | vs | NEI | 1 | 18.729 | 1.793 | 0.033 | 0.106 | 0.127 | |
| WCI | vs | SEI | 1 | 76.059 | 7.287 | 0.177 | 0.001 | 0.002 | * |
| WCI | vs | SWI | 1 | 104.763 | 11.260 | 0.220 | 0.001 | 0.002 | * |
| NEI | vs | SEI | 1 | 90.234 | 8.654 | 0.140 | 0.001 | 0.002 | * |
| NEI | vs | SWI | 1 | 138.617 | 14.349 | 0.196 | 0.001 | 0.002 | * |
| SEI | vs | SWI | 1 | 10.700 | 1.153 | 0.028 | 0.324 | 0.324 | |

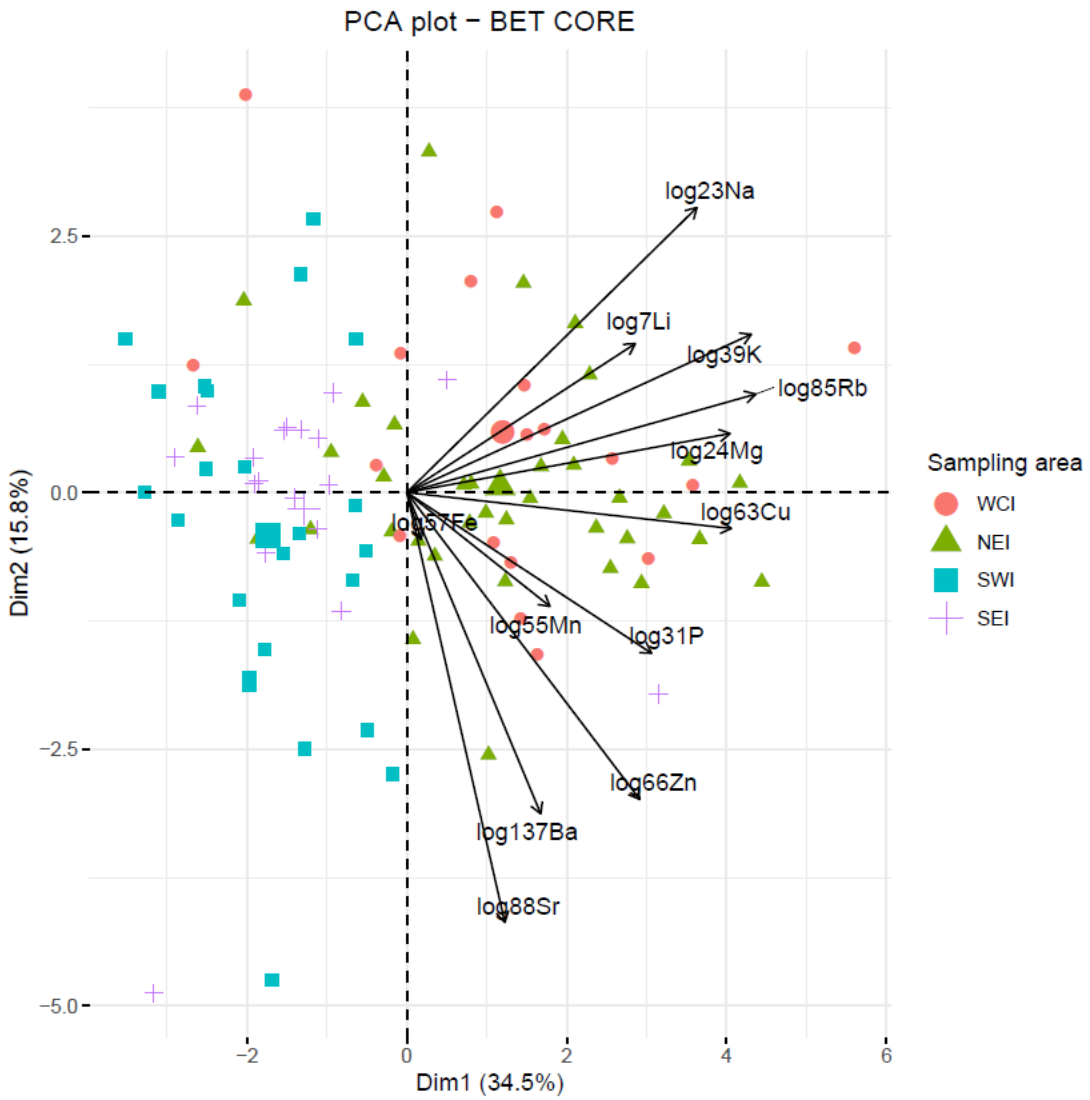


Figure 5. Biplot of individual (fish) and variable (chemical elements) projection on the first plane of the PCA made with the bigeye otolith core signatures. Individuals are coded by their sampling location. For the variables, the length of the arrow reflects the % of contribution to the total inertia.

## Edge results

Boxplots comparing edge signatures between locations for each element show that, in general, the data for the two northern locations (NEI and WCI) look similar, and likewise for the two southern locations (SEI and SWI) (Fig. 6).

The elements that contributed significantly to the interindividual variation in edge signatures (>15% to axis 1 and/or 2 in the PCA) were Ba, P, Mn and Mg. Results from PERMANOVAs run using all elements or just these four elements suggest edge signatures are not equal among all locations (p=0.001). Subsequent pairwise tests between locations show this is due to the edge signatures differing significantly between the northern and southern locations (Table 3). The edge signatures do not differ significantly between the two northern (spawning) locations, nor between the two southern locations (Table 3). Again, results using all elements are presented but the conclusions remain the same using just the subset of four elements. A biplot from the PCA showing individuals projected onto the first plane (i.e., the first two axes) helps to visualize these findings (Fig. 7).

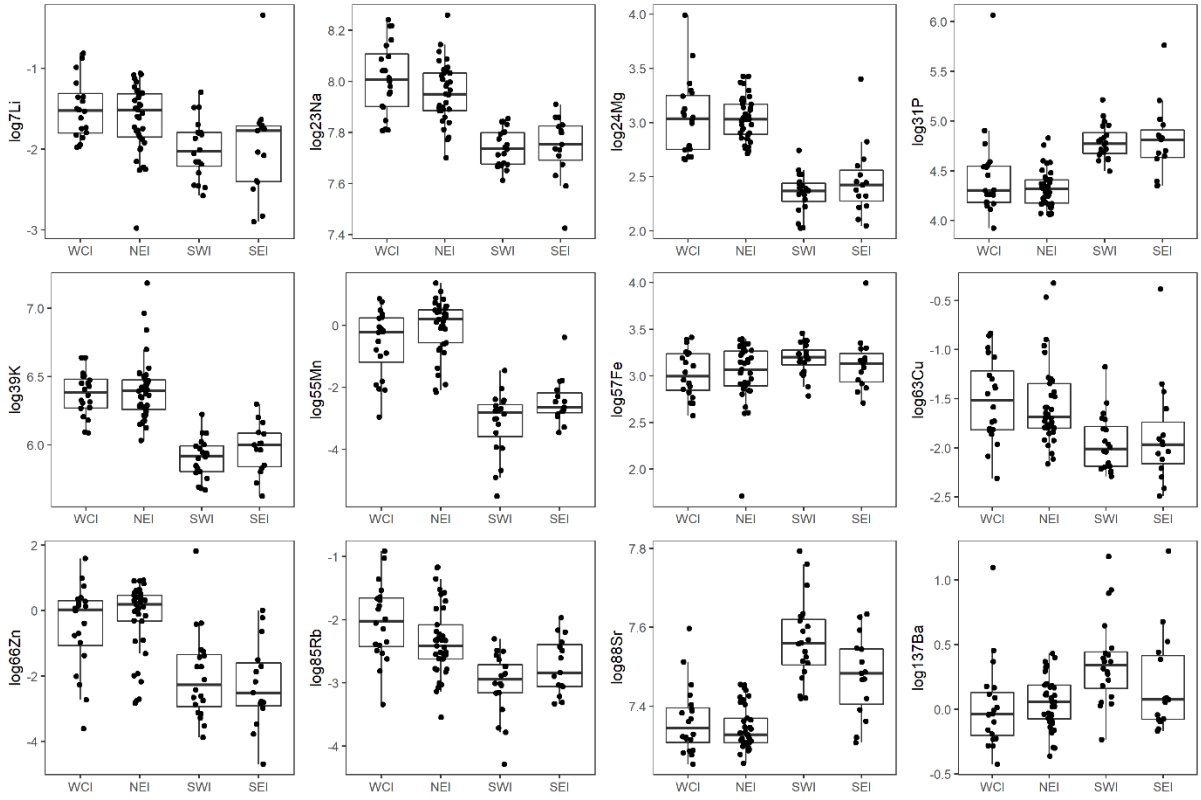


Figure 6. Boxplots comparing edge data for each element between locations. Note that the data have been log-transformed to reduce skewness and facilitate comparison.

Table 3. Results of pairwise comparisons of multi-elemental edge signatures between locations. In the Significance column, a blank means that the locations do not differ significantly at level 0.05, a dot (.) means they differ at level 0.05, and a star (*) means they differ at level 0.01.

| Pair | | | Df | Sum-of-Squares | F-statistic | R-squared | P-value | Adjusted P-value | Significance |
|---|---|---|---|---|---|---|---|---|---|
| WCI | vs | NEI | 1 | 10.174 | 1.323 | 0.023 | 0.222 | 0.222 | |
| WCI | vs | SEI | 1 | 123.875 | 12.518 | 0.275 | 0.001 | 0.002 | * |
| WCI | vs | SWI | 1 | 213.857 | 27.962 | 0.424 | 0.001 | 0.002 | * |
| NEI | vs | SEI | 1 | 155.281 | 19.843 | 0.284 | 0.001 | 0.002 | * |
| NEI | vs | SWI | 1 | 276.356 | 42.776 | 0.437 | 0.001 | 0.002 | * |
| SEI | vs | SWI | 1 | 12.359 | 1.575 | 0.046 | 0.140 | 0.168 | |

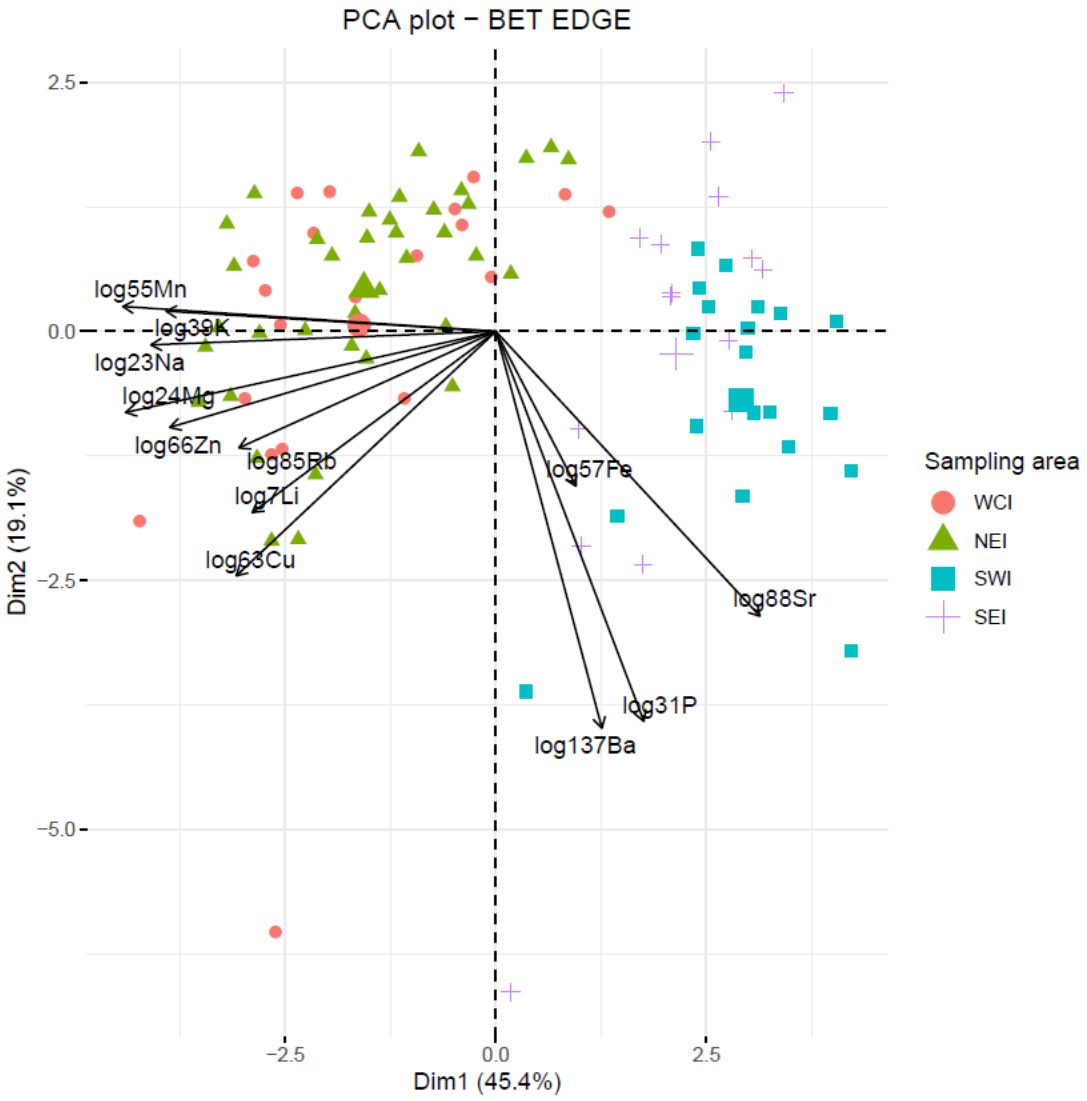


Figure 7. Biplot of individual (fish) and variable (chemical elements) projection on the first plane of the PCA made with the bigeye otolith edge signatures. Individuals are coded by their sampling location. For the variables, the length of the arrow reflects the % of contribution to the total inertia.

## Discussion

Our analyses showed that the core signatures of YOY bigeye do not differ significantly between the two northern spawning locations, suggesting either: (i) the ocean chemistry does not differ

significantly between these locations, or (ii) fish were spawned in a single location and their larvae were transported within the first few days of life to separate locations. The fact that the edge signatures also do not differ between fish from the two northern locations supports the first hypothesis, that the ocean chemistry is similar between these locations. Unfortunately, this means that these data are not useful for distinguishing which, if either, of the two northern locations adult fish sampled in the south originated from.

Interestingly, the core signatures for the southern locations do not differ significantly from each other, but they do differ significantly from the core signatures of the northern spawning locations, indicating either: (i) the fish from the south were not spawned in either of the northern locations; or (ii) they were spawned in one of the northern locations but the ocean chemistry was very different in the years they were spawned (estimated to cover a wide range from the mid-2000s to the mid-2010s) than in the years that the fish sampled from the northern locations were spawned (2017-2018). Although we cannot rule out that the ocean chemistry changed significantly between the two periods, if this were the case, we might have expected the core signatures of the southern fish to have much greater variability than the northern fish but still to overlap significantly, which is not the case (Fig. 5). In terms of edge signatures for the southern locations, they do not differ significantly from each other; given that the edge signatures should be representative of capture location, this suggests that the ocean chemistry (at least for the elements considered here) does not differ significantly between these locations.

Samples from the WCI and NEI locations were collected over 10 months, so we cannot rule out that seasonal fluctuations in oceanography over that period increased variability in the otolith signatures and that could possibly have masked spatial differentiation, i.e. the seasonal variability in the otolith signatures was greater than the variability between locations. The southern locations are subject to less seasonal variation and are more homogeneous between east and west (Davies et al 2020).

The way elements are incorporated into otoliths is influenced by age and life stage (Macdonald et al. 2020); this is clear in the otolith data for the northern locations, where even though fish are estimated to be only about 3 to 6 months old and assumed not to have undergone large-scale movements between spawning and capture, their core and edge signatures were still significantly different. However, seasonal fluctuations in oceanography within the northern spawning sites (Davies et al. 2020) may also have influenced the difference in otolith chemistry, between spawning and time of capture, within individuals.

The results show that while otolith chemistry can be used as a tool to differentiate groups of fish, temporal variability in otolith elemental chemistry may confound spatial structure information and homogeneity of the water masses hampers the application of otolith chemistry. Unfortunately, this study of elemental signatures of YOY bigeye tuna in the Indian Ocean has not provided a tool to retrospectively determine adults' natal origin, with which to infer stock structure and connectivity of this species in the Indian Ocean. Analysing YOY from known spawning areas over several years would set up a baseline for matching otolith cores from older fish collected in other areas of the Indian Ocean. In addition, incorporating data on the temporal and spatial variation in the chemical oceanography of the Indian Ocean would provide a valuable comparison with the temporal and spatial variation in otolith chemistry and, subsequently, an understanding of the extent to which oceanography influences otolith composition at different life stages. This could aid in interpretation of results including why otolith chemistry may not vary between widely separated locations, such as the two northern spawning locations in this study.

## Acknowledgements

This work was supported by funding from CSIRO Oceans and Atmosphere, AZTI Tecnalia, Institut de Recherche pour le Développement (IRD), and Indonesia's Center for Fisheries Research(CFR) and financial assistance of the European Union (GCP/INT/233/EC – Population structure of IOTC species in the Indian Ocean). The views expressed herein can in no way be taken to reflect the official opinion of the European Union. We would like to thank the many vessel owners, skippers, observers, crews and processors who provided fish for sampling and access to facilities; Thor Carter for sampling and otolith preparation; CODES staff at the University of Tasmania for providing technical advice on sample preparation and expertise in LA-ICP-MS analysis and subsequent data processing and evaluation; and Kyne Krusic-Golub and Admir Sutrovic, of Fish Ageing Services, for their expertise and adaptability in preparing otoliths from a suite of species, under time pressure.

## References

Artetxe-Arrate et al. (2019). Otolith microchemistry: a useful tool for investigating stock structure of yellowfin tuna (Thunnus albacares) in the Indian Ocean. Marine and Freshwater Research. https://doi.org/10.1071/MF19067

Campana, S. E. (1999). Chemistry and composition of fish otoliths: pathways, mechanisms and applications. *Marine Ecology Progress Series*, *188*, 263-297.

Campbell Davies, Francis Marsac, Hilario Murua, Igaratza Fraile, Zulkarnaen Fahmi, Jessica Farley, Peter Grewe, … and Achmad Zamroni. (2020). Study of population structure of IOTC species and sharks of interest in the Indian Ocean using genetics and microchemistry: 2020 Final Report to IOTC.

Evans K, Langley A, Clear NP, Williams P, Patterson T, Sibert J, Hampton J, Gunn JS. (2008). Behaviour and habitat preferences of bigeye tuna (*Thunnus obesus*) and their influence on longline fishery catches in the western Coral Sea. Can. J. Fish. Aquat. Sci. **65**(11): 2427-2443

Eveson, Paige, Julien Million, Fany Sardenne and Gaël LeCroizier. (2015). Estimating growth of tropical tunas in the Indian Ocean using tag-recapture data and otolith-based age estimates. Fisheries Research 163:58–68.

Farley JH, Clear NP, Leroy B, Davis TL and McPherson G. (2006). Age, growth and preliminary estimates of maturity of bigeye tuna, Thunnus obesus, in the Australian region. Marine and Freshwater Research. 57:713–724.

Fonteneau, A. and and Hallier, J-P (2015). Fifty years of dart tag recoveries for tropical tuna: A global comparison of results for the western Pacific, eastern Pacific, Atlantic and Indian Oceans. Fisheries Research 163 (2015) 7–22.

Hallier, J-P and Fontenau, A. (2015). Tuna aggregation and movement from tagging data: A tuna "hub" in the Indian Ocean. Fisheries Research 163 (2015) 34–43.

IOTC. (2019). Report of the 21st Session of the IOTC Working Party on Tropical Tunas. Seychelles, 21 - 26 October 2019. IOTC–2019–WPTT21–R[E]: 146 pp.

Macdonald, J. I., Drysdale, R. N., Witt, R., Cságoly, Z., & Marteinsdóttir, G. (2020). Isolating the influence of ontogeny helps predict island-wide variability in fish otolith chemistry. *Reviews in Fish Biology and Fisheries*, *30*(1), 173-202.

Nishikawa, Y., Honma, M., Ueyanagi, S. and Kikawa, S. (1985). Average distribution of larvae of oceanic species of Scombroid fishes, 1956-1981. Far Seas Fish. Res. Lab. S Ser. 12:1-99.

Norris A & Danyushevsky L (2018). 'Towards Estimating the Complete Uncertainty Budget of Quantified Results Measured by LA-ICP-MS', *Goldschmidt*, Boston, 2018-08-12.

Proctor C. H., Lester R. J. G., Clear N. P., Grewe P. M., Moore B. R., Eveson J. P., Lestari P., Wujdi A., Taufik M., Wudianto, Lansdell M. J., Hill P. L., Dietz C., Thompson J. M., Cutmore S. C., Foster S. D, Gosselin T. and Davies C. R. (2019). Population structure of yellowfin tuna (Thunnus albacares) and bigeye tuna (T. obesus) in the Indonesian region. Final Report as output of ACIAR Project FIS/2009/059.Australian Centre for International Agricultural Research, Canberra. 139 pp.

Rooker, Jay R., Jaime R. Alvarado Bremer, Barbara A. Block, Heidi Dewar, Gregorio De Metrio, Aldo Corriero, Richard T. Kraus, Eric D. Prince, Enrique Rodriguez-Marin, and David H. Secor. (2007). Life History and Stock Structure of Atlantic Bluefin Tuna (Thunnus thynnus). Reviews in Fisheries Science, 15:265–310, ISSN: 1064-1262 print DOI: 10.1080/10641260701484135.

Rooker, J. R., Wells, R. J., Itano, D. G., Thorrold, S. R., and Lee, J. M. (2016). Natal origin and population connectivity of bigeye and yellowfin tuna in the Pacific Ocean. Fisheries Oceanography 25, 277–291. doi:10.1111/FOG.12154

Sardenne, F., Dortel, E., LeCroizier, G., and Million, J. (2015). Determining the age of tropical tunas in the Indian Ocean from otolith microstructures. Fisheries163, 44–57. doi:10.1016/J. FISH RES.2014.03.008

Schaefer, K.M., Fuller, D.W., Hampton, J., Caillot, S., Leroy, B.and Itano, D. (2015). Movements, dispersion, and mixing of bigeye tuna (Thunnus obesus) tagged and released in the equatorial Central Pacific Ocean, with conventional and archival tags. Fish. Res. 161:336–355.

Stequert, B. and Marsac, F. (1989). Tropical tuna: surface fisheries in the Indian Ocean. FAO Fisheries Technical Paper, No. 282, 238p

Zudaire I., Chassot E., Murua H., Dhurmeea Z., Cedras M. and Bodin N. (2016). Sex-ratio, size at maturity, spawning period and fecundity of bigeye tuna (Thunnus obesus) in the western Indian Ocean. IOTC-2016-WPTT18-37.